Eur. Phys. J. B **4**, 45–53 (1998)

THE EUROPEAN PHYSICAL JOURNAL B

Hall effect plateaus and giant Shubnikov-de Haas oscillations in $(Bi_{0.25}Sb_{0.75})_2Te_3$ layered single crystals near the quantum limit

D. Elefant[1], G. Reiss[2], and Ch. Baier[3]

[1] Institut für Festkoerper- und Werkstofforschung Dresden, Postfach, 01171 Dresden, Germany
[2] Fakultät für Physik, Universität Bielefeld, Universitaetsstr. 25, 33615 Bielefeld, Germany
[3] FB Physik, Martin-Luther-Universität Halle-Wittenberg, Hoher Weg 7, 06120 Halle/Saale, Germany

Received: 12 September 1997 / Revised: 8 January 1998 / Accepted: 22 January 1998

Abstract. On bulk layered single crystals $(Bi_{0.25}Sb_{0.75})_2Te_3$ with a hole concentration 3.6×10^{19} cm^{-3} and a mobility $\mu = 3.7 \times 10^3$ cm^2/Vs magnetoresistance and Hall effect investigations were performed in the temperature range $T = 1.4$ K ... 20 K in magnetic fields up to 18 T. For the magnetic field perpendicular to the layered structure giant Shubnikov-de Haas oscillations are measured; the positions of the maxima are triplets in the reciprocally scaled magnetic field. From the damping of the amplitudes with increasing temperature the cyclotron mass $m_c = 0.12m_0$ is evaluated. Correlated with the SdH oscillations doublets of Hall effect plateaus (or kinks in low fields) are found. The weak well known Shubnikov-de Haas oscillations from the generally accepted multivallied highest valence band can be detected as a modulation on the giant oscillation. The high anisotropy of the SdH oscillations and their triplet structure in connection with the layered crystal structure lead us to suggest that the effects are caused by hole carrier pairing (mediated by the bipolaron mechanism) in quasi 2D sheets parallel to the crystal layer stacks. The measured Hall plateau resistances coincide with the quantum Hall effect values considering the number of layer stacks and the valley degeneracy of the 3D hole carrier reservoir. The ratio of spin splitting to Landau (cyclotron) splitting is observed to be $S = 1 \pm 0.25$.

PACS. 72.20.My Galvanomagnetic and other magnetotransport effects – 73.20.Dx Electron states in low-dimensional structures (superlattices, quantum well structures and multilayers) – 73.40.Hm Quantum Hall effect (integer and fractional)

1 Introduction

The mixed crystal system $(Bi_{1-x}Sb_x)_2Te_3$ which is applied in the field of thermoelectrics is also of special interest with respect to the fundamental influence of high magnetic fields onto the electrical conductivity in solids because of

i) its layered structure, possibly causing large anisotropy effects, and
ii) the possibility of tuning the (hole) carrier concentration in wide ranges *via* Sb–Bi–(Te) site and concentration exchange, respectively, without large lattice distortions.

Bi_2Te_3 and Sb_2Te_3 crystals have the structure of tetradymite (space group D^5_{3d}) [1], the atomic arrangement of which is most simply visualized in terms of the layer structure. Perpendicular to the trigonal c axis stacks of hexagonal layered planes are arranged, each stack consisting of five planes containing atoms of the same type according to the scheme $Te^{(1)}$–Bi(Sb)–$Te^{(2)}$–Bi(Sb)–$Te^{(1)}$. The nature of bonding is under discussion but most authors assume the bonding between the adjacent $Te^{(1)}$ layers to be of the van der Waals type. The $Te^{(2)}$ sites are sixfold coordinated, while the $Te^{(1)}$ sites have three nearest neighbours. The shorter Bi–$Te^{(1)}$ bond length compared to that of Bi–$Te^{(2)}$ is caused by an ionic bonding component in addition to the covalent bonding (for general discussion and reviews see [2,3]). The interatomic and interplanar distances of the Sb_2Te_3 and Bi_2Te_3 crystals are very similar, therefore it is possible to get mixed crystals $(Bi_{1-x}Sb_x)_2Te_3$ of very high quality. In connection with the small effective mass of the carriers and the possibility to vary their concentration there is the chance to observe galvanomagnetic quantum effects near the quantum limit in these materials.

2 Experimental

From a bulk stoichiometric $(Bi_{0.25}Sb_{0.75})_2Te_3$ single crystal, grown by the Czochralski method, two adjacent samples were prepared by a diamond saw and by cleaving with

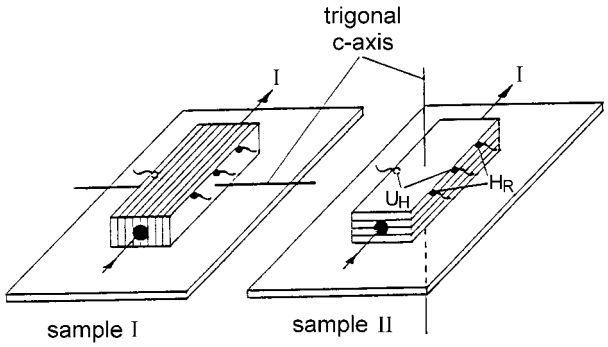

Fig. 1. Geometrical arrangement of current, resistance and Hall contacts to the trigonal axis and layered structure of the samples, respectively.

the dimensions

sample I: $16 \times 2.17 \times 0.89$ mm^3
sample II: $16 \times 1.97 \times 0.33$ mm^3

and attached to a ceramic substrate (see Fig. 1). In sample I the layer stacks are perpendicular and in sample II parallel to the substrate and to the plane of potential contact arrangement. In both cases the layer stacks are parallel to the sample length and to the electrical current. The current probes were attached to the crystals by soldering and the potential probes (40 μm thick Pt wires) by spot welding. For Hall measurements the substrates with the samples were mounted into a superconducting magnet (magnetic induction up to $B = 18$ T, temperature $T = 1.4$ K ... 20 K) perpendicular to the field direction, this way realizing $B \perp c$ for sample I and $B \parallel c$ for sample II, respectively. For magnetoresistance measurements additionally for sample II the arrangements $I \perp B \perp c$ and $I \parallel B \perp c$ were realized. For the measurements a dc technique with a sensitivity of 10^{-8} V was used. To minimize the errors caused by induction voltages due to sweeping magnetic fields and by thermovoltages the voltage drops at the Hall and resistance probes were measured at constant magnetic field for both directions and by reversing the measuring current. This way we got a discrete spectrum of absolute values of the Hall resistance and magnetoresistance.

3 Theoretical background

The well-known reason for Shubnikov-de Haas (SdH) oscillations both in three-dimensional (3D) and in two-dimensional (2D) electron systems is the orbital quantization perpendicular to a strong magnetic field B. For the energy levels of the charge carriers one obtains (see *e.g.* [4] for 2D systems):

$$E_n = E_0 + (n + 1/2)\hbar\omega_c + sg\mu_B B \tag{1}$$

with the cyclotron frequency $\omega_c = eB/m_c$, the spin quantum number $s = \pm 1/2$, the Landé factor g, and the Bohr magneton μ_B. E_0 denotes the subband bottom energy of the inversion layer (all relations and quantities are given in SI units as *e.g.* in [4]). Equation (1) is also valid for the 3D case, setting $E_0 = 0$ and adding a term for the carrier motion parallel to B. Neglecting the last term in (1) and presuming that the Fermi energy E_F and the cyclotron mass m_c do not depend on B, the Landau splitting is $\hbar\omega_c = \hbar eB/m_c|_{E=E_F}$. This gives a periodicity in $1/B$ of the density of states and therefore a corresponding periodic behavior in the galvanomagnetic properties.

Schematically including the separate spin splitting term equation (1) can be written in the form

$$E_n - E_0 = \left(n + \frac{1}{2} \pm \frac{1}{2}S\right)\hbar\omega_c \tag{2}$$

where $S = gm_c/2m_0$ is the ratio of spin splitting relative to the cyclotron splitting. By spin splitting the spin up and spin down Landau level ladders are therefore shifted relative to the Landau ladders without spin influence, causing a double set of periods in $1/B$ in the galvanomagnetic properties for constant S. A value $S > 1$ would lead to a crossing of the spin up and spin down levels originating from different quantum numbers n in (2).

The calculation of the absolute amplitudes of the SdH oscillations is complicated due to the problem of electron scattering in magnetic fields, but the damping of these amplitudes A with increasing temperature, $A \propto A_0 R_T$, provides one of the best estimates for the cyclotron mass m_c (see [5] and therein the discussion about previous publications; a detailed review of magnetic field induced oscillations including SdH oscillations is given by Shoenberg [6], and for a review of the 2D electron gas properties see [7]):

$$R_T = \frac{2\pi^2 kT/\hbar\omega_c}{\sinh(2\pi^2 kT/\hbar\omega_c)} = \frac{2\pi^2 kTm_c/\hbar eB}{\sinh(2\pi^2 kTm_c/\hbar eB)} \tag{3}$$

with ω_c as above. This relation is deduced for a 3D electron gas, but is also applicable to 2D inversion layers [8,9].

According to the Onsager relation the SdH oscillation period $\Delta(1/B)$ is inversely proportional to the extremal cross sectional area $A_\perp$ (perpendicular to B) of the Fermi surface $\Delta(1/B) = 2\pi e/\hbar A_\perp$. For a parabolic dispersion the relation between the SdH period $\Delta(1/B)$ and the carrier concentration n is

$$\text{3D:}\ \Delta(1/B) = \frac{2e}{\hbar}(g_s g_\nu/6\pi^2 n)^{2/3} \tag{4a}$$

$$\text{2D:}\ \Delta(1/B) = \frac{e}{2\pi\hbar}(g_s g_\nu/n) \tag{4b}$$

with g_s and g_ν the spin and valley degeneracy factors, respectively.

4 Results and discussion

4.1 Hall plateaus and giant oscillations

Figure 2 shows the Hall resistivity $\rho_{xy} = dU_H/I$ (d sample thickness) for $B \perp c$ up to $B = 16$ T and for $B \parallel c$ up to $B = 18$ T, respectively. In the first case we see a

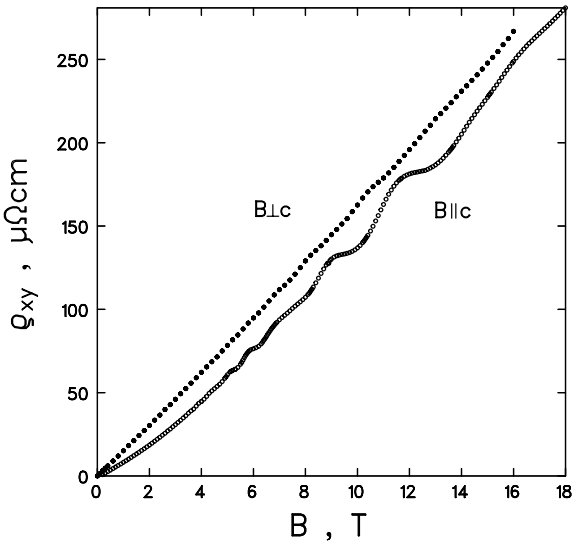

Fig. 2. Hall resistivity ρ_{xy} as a function of the magnetic field B at $T = 1.4$ K; the direction of B is parallel to the trigonal axis ($B \parallel c$, open circles) and perpendicular to the trigonal axis ($B \perp c$, filled circles).

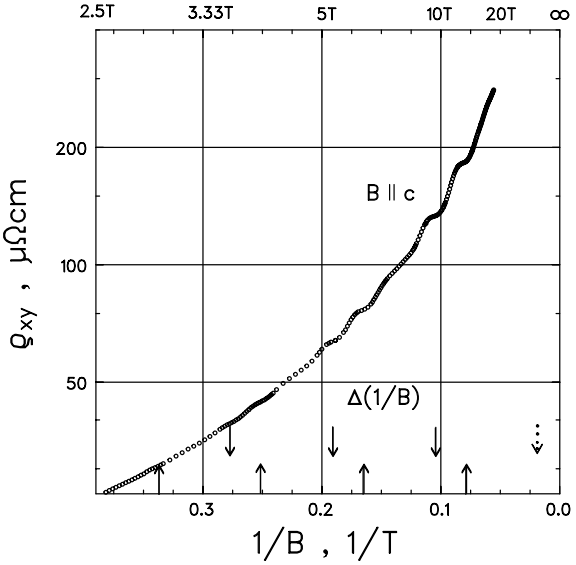

Fig. 3. Hall resistivity ρ_{xy} for $B \parallel c$ as a function of the inverse magnetic field $1/B$. The arrows mark the positions of the Hall plateaus, showing two sets of equal periods. The dashed arrow is the extrapolation to the highest field region (see text). In the lower set an extrapolation is not possible, showing that the last Landau level is reached.

nearly constant slope of the Hall resistivity, whereas for $B \parallel c$ remarkable plateaus or kinks are visible. The average slopes of the ρ_{xy} *versus* B curves $R_H = \Delta\rho_{xy}/\Delta B$ in both cases are almost identical (for $B \geq 4T$), leading to a p-type carrier concentration

$$n_H = (eR_H)^{-1} = 3.6 \times 10^{19}\ \mathrm{cm}^{-3} \tag{5}$$

independent from current and magnetic field direction to the crystal axes, respectively.

Figure 3 shows the Hall resistivity ρ_{xy} for $B \parallel c$ in a $\log(\rho_{xy})$ *versus* $1/B$ representation, with arrows marking the centres of the Hall plateaus. We find doublets with a period in $1/B$:

$$\Delta(1/B) = (0.086 \pm 0.002)\ \mathrm{T}^{-1}. \tag{6}$$

The extrapolation of the $\Delta(1/B)$ periods towards highest fields leads for the set of periods marked with $\downarrow$ arrows in Figure 3 to a value $B \cong 40$ T (dashed arrow in Fig. 3), whereas for the other set (marked with $\uparrow$ arrows) an extrapolation is not possible for finite fields, demonstrating that the last Landau level is reached (compare Fig. 9).

Figure 4 shows the magnetoresistivity ρ_{xx} for the two samples for the configurations $I \perp B \perp c$ (samples I and II), $I \parallel B \perp c$ and $I \perp B \parallel c$ (sample II, see also Fig. 1). The magnetoresistivity ρ_{xx} for all cases with $B \perp c$, after raising with field, tends to saturation with small superimposed oscillations for high fields, whereas for the configuration $B \parallel c$ in fields $B > 5$ T we observe giant oscillations, the amplitudes of which are at least an order of magnitude larger than for the cases $B \perp c$.

A closer look to the large oscillation in Figure 4 shows that it is weakly modulated (*e.g.* at $B \cong 15$ T). To show this modulation the second derivative of the resistivity

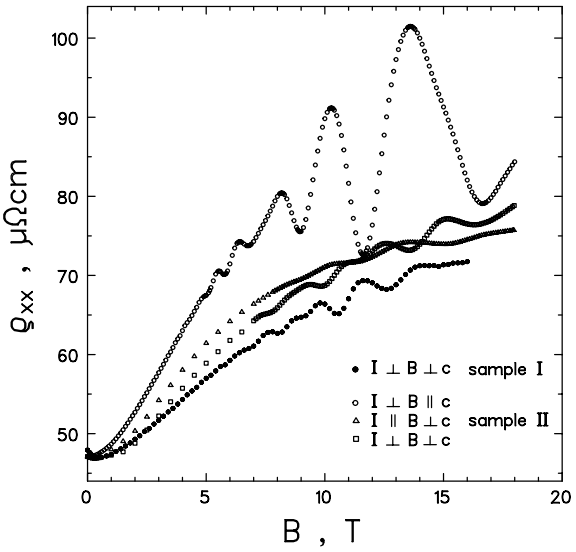

Fig. 4. Magnetoresistivity ρ_{xx} *versus* magnetic field B for different configurations of current I, magnetic field B and trigonal axis c for the two samples at $T = 1.4$ K (see Fig. 1).

with respect to B (from a measurement with enhanced density of experimental values) is shown *versus* $1/B$ in Figure 5.

From the results shown in Figures 2 and 4, we can estimate a hole carrier mobility $\mu = R_H\sigma$ to $\mu \cong 3.7 \times 10^3$ cm^2/Vs leading to $\mu B = \omega_c\tau \cong 6$ for $B = 16$ T, demonstrating that we reach with our material and the available magnetic fields the high field limit (the residual resistance ratio amounts to $\rho(300K,\ B = 0)/\rho(1.5K, B = 0) = 10.6$).

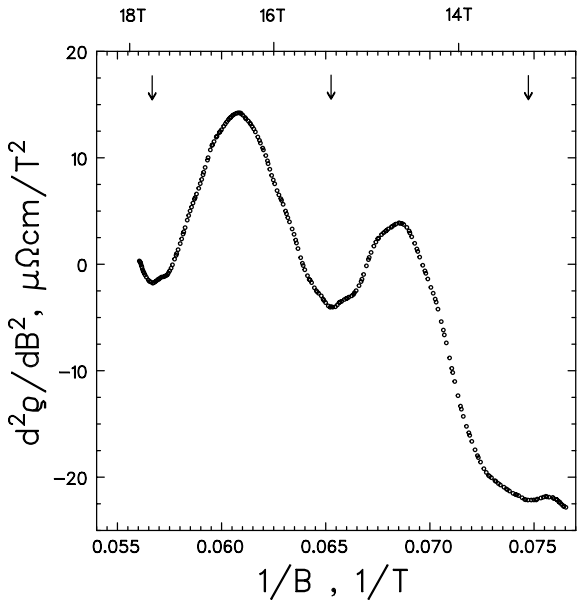

Fig. 5. Second derivative of the magnetoresistivity $d^2\rho_{xx}/dB^2$ *vs.* reciprocal magnetic field $1/B$ of the giant ρ_{xx} oscillation in Figure 4 (open circles) for enhanced density of experimental values ($B \parallel c$, $T = 1.4$ K).

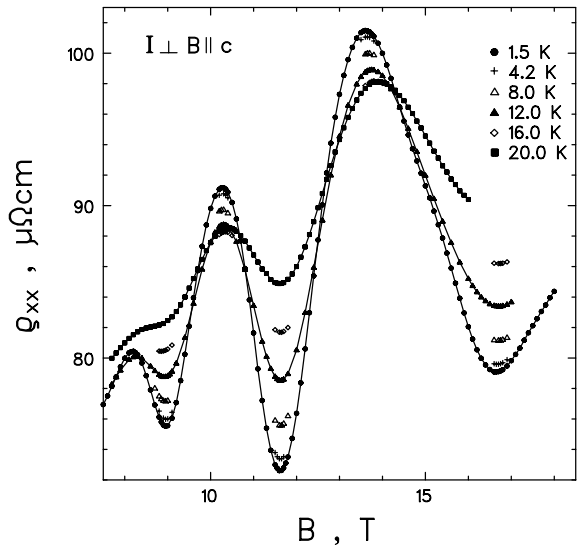

Fig. 6. Temperature dependence of the ρ_{xx} oscillation (see Fig. 4, open circles) for $B \parallel c \perp I$.

Figure 6 shows the temperature dependence of the giant oscillations $B \parallel c$ from Figure 4 for temperatures in the range $T = 1.4$ ... 20 K. It is remarkable, that in the temperature range $T = 1.4$ ... 4.2 K the damping is very weak and that even at $T = 20$ K the oscillations are far from being damped out. The estimation of the cyclotron mass m_c for a fixed magnetic field B was done as follows: for the most pronounced oscillation minima in Figure 6 at $B \cong 11.6$ T the maximum amplitudes for this field were interpolated from the neighbouring maxima at $B \cong 10.3$ T and $B \cong 13.6$ T, respectively (see *e.g.* [10]). The resistivity differences between these interpolated values and

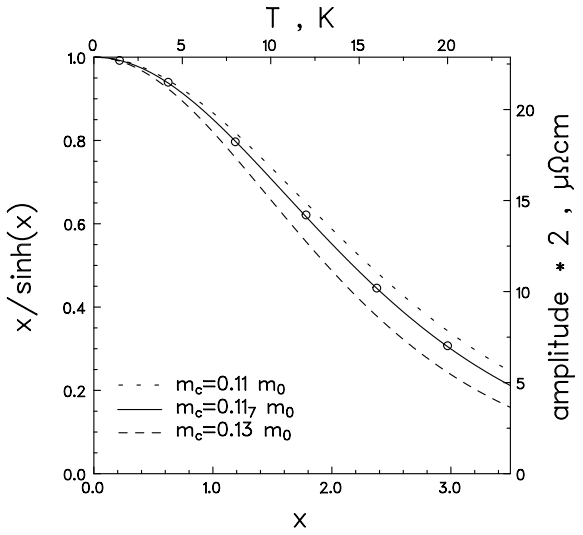

Fig. 7. Amplitude of the SdH oscillation at $B = 11.63$ T in dependence on the temperature (open circles, related to the right and the upper scale). The lines are the calculated curves $x/\sinh(x)$ with $x = 2\pi^2 kT/\hbar\omega_c = 2\pi^2 kTm_c/\hbar eB$ for different m_c values (see Eq. (3)). The sketched x scale relates to $m_c = 0.117m_0$, for other m_c values this scale has to be corrected by the factor $m_c/0.117m_0$ (see Fig. 6 and text).

the measured minima are drawn in Figure 7 (circles) as 2×amplitude related to the the temperature scale. Fitting these points to the oscillation temperature damping factor R_T (Eq. (3)) delivers a cyclotron mass $m_c = 0.117m_0$ of the carriers. This value is larger than the published one $m_c \approx 0.09m_0$ [19], but the authors admit considerable uncertainties because they measure very small amplitudes.

4.2 Correlation between Hall resistivity and SdH oscillations

Figure 8 shows the Hall resistivity ρ_{xy} and the magnetoresistivity ρ_{xx} in dependence on the magnetic field from 5 T to 18 T. The following features are remarkable:

i) the plateaus in the Hall resistivity ρ_{xy} begin to appear at a magnetic field where the resistance ρ_{xx} has a minimum, and they vanish, when ρ_{xx} has a maximum value;
ii) between the ρ_{xy} pairs of plateaus marked in Figure 8 (see also Fig. 3), we see additionally a minimum and a maximum in ρ_{xx} (see dashed square in Fig. 8), not accompanied by a pronounced plateau of ρ_{xy}.

The unambiguous correlation between ρ_{xx} and ρ_{xy} on the one hand and the characteristic differences in the shape of the Hall resistivity plateaus on the other hand show, that for the period $\Delta(1/B)$ of the SdH oscillations the value (6) holds, too, and not a very smaller one as it could be the impression at first glance, looking only at Figure 4.

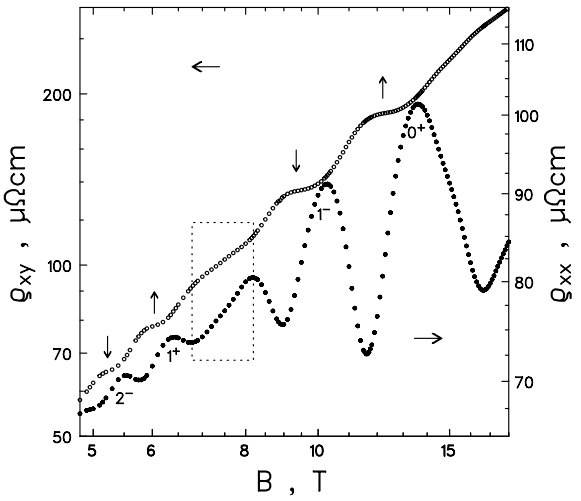

Fig. 8. Hall resistivity ρ_{xy} (open circles, left scale) and magnetoresistivity ρ_{xx} (filled circles, right scale) as a function of the magnetic field B (in log scales) for $B \parallel c$ and $T = 1.4$ K (for the notations of the resistivity maxima see Fig. 9 (left diagram) and Sect. 4.2).

Table 1. Magnetic field strengths (error $\Delta B = 0.03$ T) at the maximum values of the SdH oscillations; the row arrangement corresponds to the correlation with the Hall plateaus of kinks (See Figs. 3 and 8).

kind of maximum	B_{maxSdH}/T			
↑	13.60	6.40	4.12	3.08
		8.15	4.73	3.30
↓		10.28	5.51	3.70

4.3 Spin splitting

From the $1/B$-periods of the Hall plateaus in Figure 3 we conclude with relations (1) and (2), respectively, that the charge carriers have a unique cyclotron mass but they are spin split. In order to estimate the spin splitting with respect to Landau splitting in relation (2) we use the B-positions of the conductivity oscillation maxima, since a Landau level passing through the Fermi surface causes a maximum in the conductivity σ_{xx}. The relation between the measured values ρ_{xx} and ρ_{xy} with σ_{xx} and σ_{xy} is

$$\rho_{xx} = \frac{\sigma_{xx}}{\sigma_{xx}^2 + \sigma_{xy}^2}; \quad \sigma_{xx} = \frac{\rho_{xx}}{\rho_{xx}^2 + \rho_{xy}^2} \cdot \tag{7}$$

The results are collected in Table 1, showing the B values for the σ_{xx} maxima of the SdH oscillations.

Figure 9 gives the positions of the SdH-maxima (thick lines) as a term scheme in a $1/B$ scale for two possible combinations of the spin split terms and the Landau splitting on the basis of relation (2) (compare [6], p. 425, especially for the problem of the shown ambiguity of term coordination).

i) Instead of the doublets in the Hall plateaus, the SdH-oscillations arrange in a triplet structure, where the lowest and the highest terms of a triplet are correlated with the pronounced Hall plateaus or kinks (Fig. 3), whereas the middle term is only correlated with the mentioned slightly decreased slope of the Hall resistivity (see Fig. 8 and Sect. 4.2).
ii) Taking into account only the upper and lower terms we get for the ratio S of spin to cyclotron splitting for both term combinations of Figure 9 the ambiguous value $S = 1 \pm 0.25$.
iii) A decision between the two possible term schemes of Figure 9 can only be obtained by extending the measurements to magnetic fields $B \cong 40$ T, *i.e.* the detection of the term labelled with 0^-. Because of the slight increase of the splitting with decreasing magnetic field in the right diagram and, reversed, a slight decrease of splitting in the left diagram of Figure 9 we favour the left term coordination, the term labels of which (quantum number n and sign of spin splitting in Eq. (2)) are also used in Figures 8 and 10.
iv) Figure 9 shows that the lowest Landau level for one spin direction is reached.
v) Angular dependent measurements of the SdH oscillations [11] show, that tilting of the magnetic field with respect to the trigonal axis c drastically influences amplitudes and frequency, not compatible with the simple replacing of B by $B_\perp$ for Landau splitting and unchanged B for spin splitting ($B_\perp = B\cos\Theta$ with Θ being the tilt angle), as it works *e.g.* for inversion layers [9].

For the analysis of oscillations in magnetic fields often a diagram as Figure 10 is used (see *e.g.* [6,10,21]. Integers (corresponding to units of π or 2π of the oscillation frequency) are attributed to the $1/B$ values of maxima, minima or crossings with the mean line of the oscillations, this way showing frequency changes as deviations from a straight line. The ordinate intercept of the extrapolated curve for $1/B = 0$ corresponds to the phase of the oscillations. In our case we took the oscillation maxima and used the Landau level notation from Figure 9, left diagram. As Figure 10 shows we find within the experimental accuracy nearly equidistant straight lines for our triplet term structure from Figure 9. Except the dashed values, the existence of which will be discussed later, equation (2) with constant S and m_c is confirmed.

4.4 Comparison with published results

The Brillouin zone of Bi_2Te_3 resulting from the tetradymite structure was sketched and discussed elsewhere [12,13]. Band structure calculations agree in the prediction of a six valley type conduction band (but with different positions of the corresponding Fermi surface ellipsoids in the mirror planes of the Brillouin zone), whereas the valence band may contain either three or six valleys [13–15]. SdH measurements concerning the valence band are published *e.g.* for p-Bi_2Te_3 [16,17], p-Sb_2Te_3 [18], and the mixed system p-$(Bi_{1-x}Sb_x)_2Te_3$ [19] with the following aspects important for the discussion of our

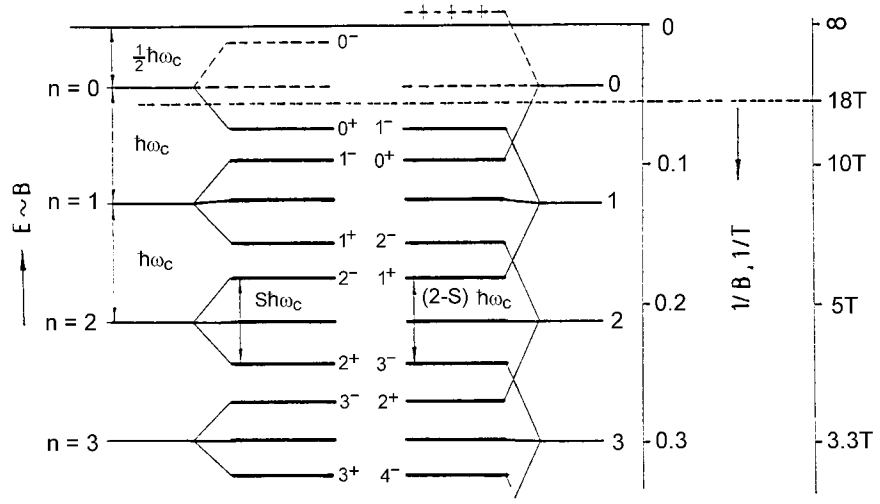

Fig. 9. Possible schemes of Landau (cyclotron) level spacings $\hbar\omega_c$ with the measured spin split level spacings (thick lines) as a function of $1/B$ (right scale) (see text).

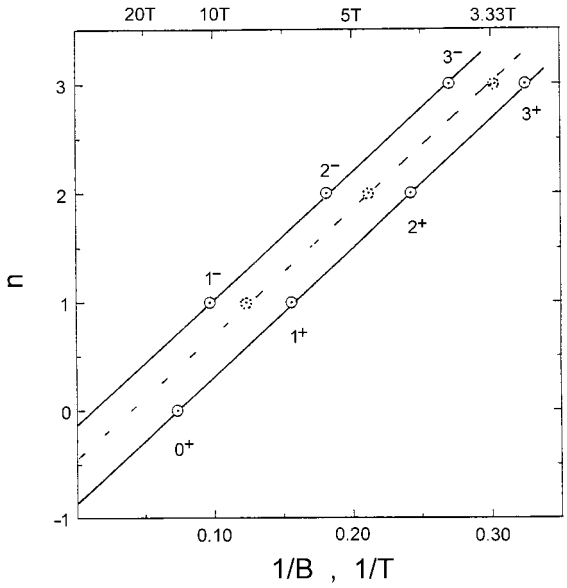

Fig. 10. Integer values n, attributed to the measured giant SdH maxima according to relation (2) and Figure 9 (left) with Table 1, *versus* the corresponding $1/B$ values (the SdH maxima without clear Hall plateaus are marked by dashed circles, comp. Fig. 8)

measurements:

i) The authors postulate a six valley (or 12 valley [18]) valence band. Because of the arrangement of the corresponding Fermi surface ellipsoids pairwise in the three mirror planes of the Brillouin zone in general three different extremal cross sections $A_\perp$ of these ellipsoids create with $\Delta(1/B) = 2\pi e/\hbar A_\perp$ three SdH periods. Only for $B \parallel c$ (c: trigonal axis) one single oscillation period is observed. All oscillations may be spin split.

ii) No absolute values of the oscillation amplitudes are published, but it is stated, that for hole concentrations $p > 10^{19}$ cm^{-3} in p-Bi_2Te_3 the SdH amplitudes ($B \parallel c$) are small and hence the accuracy of the m_c determination is poor [16]. For the system p-$(Bi_{1-x}Sb_x)_2Te_3$ for $x > 0.6$ very small SdH amplitudes are reported and for $x \geq 0.8$ no spin splitting is observed [19]. In no case a remarkable dependence oft the amplitude on the direction of the magnetic field is reported.

iii) Increasing the hole concentration above $p_H = 3 \times 10^{18}$ cm^{-3} leads to discrepancies between the Hall data and the SdH periods (compare Eq. (4a)). These problems are attributed to the filling of a second valence band.

4.5 Discussion

With respect to the published results, our measurements can be interpreted as follows:

i) the measured relatively small oscillations for $B \perp c$ (Fig. 4), which are not correlated with plateaus or kinks in the Hall resistivity (Fig. 2) and the superimposed weak oscillation for $B \parallel c$ (Fig. 5) are bulk SdH oscillations well-known from literature in the system $Bi(Sb)_2Te_3$ [16–19];

ii) the giant oscillations for $B \parallel c$ which are correlated with Hall plateaus can be considered as a sort of a quantized Hall effect (QHE) in our layered material.

Hall effect plateaus and correlated giant SdH oscillations are well-known features of a strictly 2D electron gas in a magnetic field, first realized in inversion layers of MosFets [20]. Our material, however, is a bulk single crystal with a highly anisotropic layered structure.

The occurrence of the QHE in an anisotropic three dimensional electronic system was proved in [21]. *Via* MBE a GaAs/(AlGa)As superlattice structure was grown containing 30 quantum wells with well thicknesses of 188 Å and thin barriers of 38 Å. The QHE found in this system coexists with a three dimensional dispersion of the electrons. The values of the QHE plateaus ρ^i_{xy} can be expressed with a 25% accuracy as $\rho^i_{xy} = \frac{1}{i}\frac{h}{e^2}\frac{1}{j}$, with i being the usual counter of the QHE plateaus; j equals the number of quantum wells and thus $1/j$ simply takes into

account that j QHE layers form a parallel circuit in the quantum well system. It is argued that because of the dispersion perpendicular to the barriers each Landau level is broadened from a δ function to a band which reflects the 1D density of states in this direction. With a Kronig-Penney model for computing the dispersion perpendicular to the barriers most of the features could be explained quantitatively.

In analogy to this system one could regard our layered material as a multiple quantum well structure: each layer stack separated by ultrathin barriers in the planes where van der Waals bonding acts. But calculations with a Kronig-Penney model (parameters: $m^* = 0.12m_0$ from Fig. 7, well width $a = 7.4$ Å and barrier width $b = 2.7$ Å as for our layer stacks [2,3], barrier height $V = 50$ ... 500 meV) deliver no remarkable deviation from a simple parabolic dispersion with the above m^* for the direction perpendicular to the layer structure, *i.e.* the van der Waals bonds of the layers cannot produce a connected multiple quantum well structure in the crystal. The concept of a superlattice-like structure of our material therefore fails to explain the QHE like phenomena.

In order to clarify the origin of the giant SdH oscillations and the related Hall plateaus and kinks found in our material we state the following results.

i) The features occur only for $B \parallel c$ and $I \perp c$, *i.e.* there is a large anisotropy which shows a 2D behavior (Fig. 4).
ii) The carrier concentration obtained from the periods $\Delta(1/B)$ for the 3D case (Eq. (4a)) is more than one order of magnitude smaller than that one calculated from the slope of the ρ_{xy} *versus* B curve. An explanation of the measured effect within a 3D-scheme therefore fails.
iii) The values of $(1/B)$, where the SdH maxima are found fit in a scheme of triplets (Fig. 9) which cannot be correlated with charge carriers having spin $s = \pm 1/2$ but with $S = 1, 0, -1$. This points to electron (hole) pairs being responsible for the large SdH oscillations in the layer planes.

We therefore suggest, that a mechanism active within the layer stacks of the material leads to a partial 2D electron (hole) pairing in the planes sandwiched between van der Waals bonds.

Since years carrier pairing mechanisms are widely under discussion in connection with the high temperature superconductivity (for a short review see *e.g.* [22]). Among them the bipolaronic pairing should be favoured by a low dimensional structure, mixed valence states of one sort of atoms, and a low carrier density (for a detailed review see [23]). The properties of our material meet these points (see also Sect. 1). The bipolaronic mechanism is based on a concept of pairing in real space. The bipolarons should align themselves along chains in the material of lower dimensionality, whereby the attractive interaction can overcome the Coulomb repulsion of the two carriers only for a small distance [24].

We therefore conclude, that the carrier pairing in our material should be parallel to each layer stack in real space, resulting in a set of j nearly 2D sheets of paired carriers in a 3D electronic system (with j the number of layer stacks in our sample).

This model can explain the main features of our measurements.

i) In the bipolaron model the triplet structure of Figure 9 corresponds to "near neighbor site" bipolarons (Heitler London pairs).
ii) Computing n for a 2D sheet after (4b) with the oscillation period (6) and a valley degeneracy $g_\nu = 3$ (Sect. 4.4, [7,13,15]), adding for all layer stacks (10.1 Å stack thickness and 0.33 mm sample thickness corresponding to 3.3×10^5 stacks) and considering the triplet structure of the oscillations (Fig. 9) we get a carrier concentration $n_{2D} = 2.5$ ... 2.6×10^{19} cm^{-3}. This should be the fraction of the carrier concentration involved in 2D pairing.
The same value is obtained with the well-known expression for the degeneracy of a Landau level $n = eB/h$ (see *e.g.* [4]), taking for B the value of the pronounced minimum $B = 11.63$ T (Figs. 4 and 6) and counting three occupied Landau levels corresponding to the left diagram in Figure 9 (valley degeneracy, number of sheets and sample geometry as above).
The difference n_1 to the total concentration $n_H = 3.6 \times 10^{19}$ cm^{-3} derived from the Hall data (5), $n_1 = n_H - n_{2D}$, then is the reason for the weak upword modulated bulk SdH oscillation from Figure 5. Taking the relation SdH period $\Leftrightarrow$ carrier concentration (4a) in the adjacent system p-Sb_2Te_3 [18] as comparison for our material, n_1 is nearly confirmed by the oscillation period in Figure 5.
iii) Presuming two "groups" of carriers – one of them involved in 2D carrier pairing and showing plateaus in the Hall effect and the other one showing 3D behavior – the measurement should reflect their properties in parallel, *i.e.* the resulting Hall resistivity is lower than that ones of the single carrier groups and *e.g.* the plateaus of the 2D carrier group are smeared out. Using the relation $\frac{1}{\rho_{xy}} = \frac{1}{\rho_{xy}^{2D}} + \frac{1}{\rho_{xy}^{3D}}$ which should be applicable after [25] for two carrier groups in the high field limit we calculated the Hall resistivity ρ_{xy}^{2D} from the measured values ρ_{xy} (with $\rho_{xy}^{3D} = B/en_{1(3D)}$ and $n_{1(3D)} = n_H - n_{2D}$ the difference between the total carrier concentration n_H (5) and n_{2D} as above).
The result is shown in Figure 11 (open circles) in comparison to the measured values (filled circles). The right ordinate axis is scaled in units of the measured Hall resistance $R_{Hall} = U_{Hall}/I$ (U_{Hall}: Hall voltage, I: measuring current), whereas the left ordinate is scaled in units of the (bulk) Hall resistivity $\rho_{xy} = R_{Hall}d$; ($d = 0.33$ mm sample thickness).
If the model of 2D carrier sheets within the crystal planes works, then the corresponding Hall resistance R_{Hall}^{2D} should result from the connecting in parallel of the $j = 3.3 \times 10^5$ layer stacks (thickness of the stacks 1.01 nm [2,3] in our material). Considering as above a valley degeneracy $g_\nu = 3$ we get for the resulting Hall

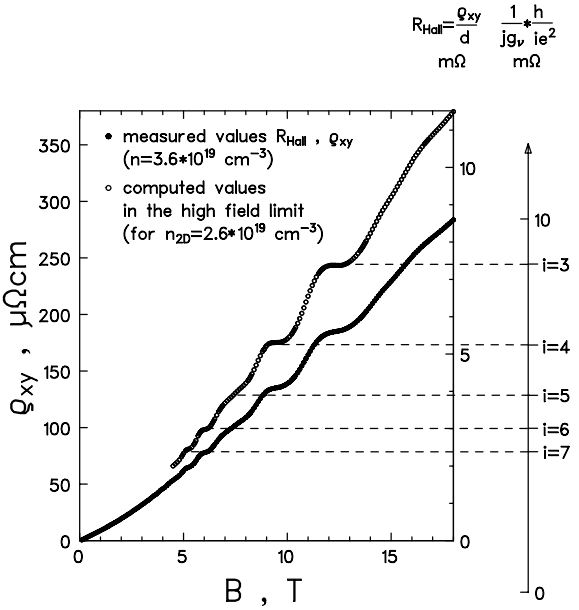

Fig. 11. Hall resistance or Hall resistivity, respectively, for $B \parallel c$ and $T = 1.4$ K (filled circles: measured values; open circles: computed values in the high field limit for the fraction of holes assumed to be paired; see text). The second right ordinate scale shows the QHE plateau values $R^i_{Hall} = \frac{1}{g_\nu}\frac{1}{j}\frac{h}{ie^2}$ for j parallel 2D carrier sheets and a valley degeneracy g_ν ($j = 3.3\times10^5$; $g_\nu = 3$; $i = 3$ ... 7).

plateau values

$$R^i_{Hall} = \frac{1}{g_\nu}\frac{1}{j}\frac{h}{ie^2} \qquad (8)$$

with the Klitzing value $h/e^2 = 25.812$ ... kΩ.
In Figure 11 these values for $i = 3$ ... 7 are sketched on an additionally ordinate axis on the right side. It is obvious that the absolute values can not coincide because the simple calculations according to the two band model are nearly correct only in the high field limit, whereas for low fields the Hall resistance is generally underestimated. Shifting this axis downward in the shown way the plateau values of the "2D carriers" coincide with the quantized Hall effect values after (8), this way showing that the differences of the plateaus are in agreement with the QHE. Independent from the question whether the assumed valley degeneracy is correct and if one can accept the proposed carrier separation the correct order of magnitude of the quantized Hall plateaus is met by the suggestion, that the number of parallel 2D carrier sheets corresponds to the number of layer stacks in our sample.

Up to now QHE like behavior in bulk crystals is observed in some salts of the organic TMTSF molecule (well known as organic superconductors) under partly difficult experimental conditions as high pressure (for a review see [26]). As reason for the QHE plateaus in this system semimetallic FISDW (field induced spin density wave) phases, coupled to the layer structure, are thought to be responsible.

Giant SdH oscillations (without Hall plateaus) are reported on certain phases of the salts of the organic BEDT-TTF molecule (see *e.g.* [27] for β-(BEDT-TTF)$_2$I$_3$). They are attributed to the warped cylindrical Fermi surface caused by the layered structure of the material.

Magnetization measurements in high fields at α-(BEDT-TTF)$_2$TlHg(SCN)$_4$ indicate the presence of deep minima in the transverse magnetoresistivity, the behavior of which is explained quantitatively in terms of enhanced conductivity due to the QHE [28].

As pointed out above – supported mainly by the triplet structure of the SdH oscillations and their correlation to the Hall plateaus – we state that in our anorganic crystalline material a different mechanism produces QHE and giant SdH oscillations. Independent from the differences a layered structure seems to be the common prerequisite to observe QHE in 3D materials.

5 Conclusions

In summary, we have shown that the holes in the investigated $(Bi_{0.25}Sb_{0.75})_2Te_3$ layered crystal produce SdH oscillations and plateaus of the Hall resistance which are in strong contradiction to previous reports if the the magnetic field is perpendicular to the layer planes.

In this case, very large SdH oscillations correlated with plateaus and kinks in the Hall resistance were measured. The damping of the SdH amplitudes with increasing temperature gives a cyclotron mass of $0.12m_0$, about 30% larger than in published results.

The evaluation showed, that the periods of the SdH oscillations and the related Hall resistivity matches a scheme of a triplet structure. In addition, the occurence of Hall plateaus, the large amplitudes of the SdH oscillations, and the relation of their periods with the carrier concentration led us to suggest the existence of carrier pairing in the quasi 2D sheets of the layered crystal structure.

This 2D layered structure, the existence of atoms of one sort with different valence states and the relative low carrier density are favourable circumstances for the bipolaron model to be the relevant carrier pairing mechanism. Taking the suggested structure of parallel 2D sheets of paired carriers coupled to the crystal layer stacks we obtained a good coincidence of the Hall plateaus with the values of the quantized Hall effect.

The authors gratefully acknowledge the help of L.D. Ivanova (BAIKOV Institute of Metallurgy, Moscow) for supplying the high quality single crystal and the cooperation of A. Heinrich, P. Verges, and H. Vinzelberg. We are indebted to S.L. Drechsler for directing the authors' attention to the bipolaron pairing model and to Mrs. I. Kiwitz for technical assistance.

References

1. A. Krost, in *Landoldt-Börnstein, Neue Serie Band 17*, edited by O. Madelung, M. Schulz, H. Weiss (Springer Verlag, Berlin/Heidelberg/New York/Tokyo 1983), p. 234.
2. N.Kh. Abrikosov, V.F. Bankina, L.V. Poretskaya, L.E. Shelimova, E.V. Skudnova, *Monographs in Semiconductor Physics*, Volume 3: Semiconducting II-VI, IV-VI, and V-VI Compounds (Plenum Press, New York, 1969), pp. 159-246.
3. F. Hulliger, *Structural Chemistry of Layer-Type Phases*, edited by F. Levy (D. Reidel Publishing Company, Dordrecht-Holland/Boston, USA, 1976), pp. 196-201.
4. K. von Klitzing, Rev. Mod. Phys. **58**, 519 (1986).
5. E.N. Adams, T.D. Holstein, J. Phys. Chem. Solids **10**, 254 (1959).
6. D. Shoenberg, *Magnetic oscillations in metals* (Cambridge University Press, 1984).
7. T. Ando, A.B. Fowler, F. Stern, Rev. Mod. Phys. **54**, 437 (1982).
8. A.B. Fowler, F.F. Fang, W.E. Howard, P.J. Stiles, Phys. Rev. Lett. **16**, 901 (1966).
9. F.F. Fang, P.J. Stiles, Phys. Rev. **174**, 823 (1968).
10. R.J. Sladek, Phys. Rev. **110**, 817 (1958).
11. D. Elefant *et al.*, to be published.
12. R.B. Mallinson, J.A. Rayne, R.W. Ure, Phys. Rev. **175**, 1049 (1968).
13. R. Togei, G.R. Miller, in *The Physics of Semimetals and Narrow Gap Semiconductors*, edited by D.L. Carter, R.P. Bate (Pergamon Press, 1971), p. 349.
14. E. Borghese, E. Donato, Nuovo Cimento **53**, 283 (1968).
15. S. Katsuki, J. Phys. Soc. Jpn **26**, 58 (1969).
16. H. Köhler, Phys. Stat. Sol. (b) **74**, 591 (1976); H. Köhler, Phys. Stat. Sol. (b) **75**, 441 (1976).
17. A. von Middendorff, G. Landwehr, Solid State Commun. **11**, 203 (1972).
18. A. von Middendorff, K. Dietrich, G. Landwehr, Solid State Commun. **13**, 443 (1973).
19. H. Köhler, A. Freudenberger, Phys. Stat. Sol. (b) **84**, 195 (1977).
20. K. von Klitzing, G. Dorda, M. Pepper, Phys. Rev. Lett. **45**, 494 (1980).
21. H.L. Störmer, J.P. Eisenstein, A.C. Gossard, W. Wiegmann, K. Baldwin, Phys. Rev. Lett. **56**, 85 (1986).
22. J. Ashkenazi, C.G. Kuper, in *Studies of High Temperature Superconductors. Advances in Research and Applications*, Vol. 3, edited by N. Narlikar (Nova Science Publishers, Commack, NY, USA, 1989), p. 1.
23. R. Micnas, J. Ranninger, S. Robaszkiewicz, Rev. Mod. Phys. **62**, 113 (1990).
24. B.K. Chakraverty, Philos. Mag. **42**, 473 (1980).
25. C.M. Hurd, *The Hall Effect in Metals and Alloys* (Plenum Press, New York, London, 1972), p. 87.
26. D. Jérome, Solid State Commun. **92**, 89 (1994).
27. W. Kang, G. Montambaux, J.R. Cooper, D. Jérome, P. Batail, C. Lenoir, Phys. Rev. Lett. **62**, 2559 (1989).
28. N. Harrison, A. House, M.V. Kartsovnik, A.V. Polisski, J. Singleton, F. Herlach, W. Hayes, N.D. Kushch, Phys. Rev. Lett. **77**, 1576 (1996).